Characterization of liquid adsorption columns by computed tomography

Dirk-Uwe Astrath[1], Duc Thoung Vu[2], Wolfgang Arlt[1], Erling Stenby[2]

[1] Chair of Separation Science & Technology, Chemical and Bioengineering in Erlangen, Friedrich-Alexander University Erlangen-Nuremberg

[2] Center for Phase Equilibria and Separation Processes, Department of Chemical Engineering, Technical University of Denmark

Introduction

The efficiency of liquid adsorption and especially chromatographic columns strongly depends on a homogeneous structure of the packing, e.g. an evenly distributed interstitial void fraction. Evidences that the structure of the packed bed is not necessarily homogeneous can be found in the literature. The inhomogeneities of the packing can either be a consequence of the packing process or are caused by the operation of the column. In either case they lead to maldistributions of the mobile phase flow and a deterioration of the separation efficiency. Commonly, the efficiency of adsorption and chromatographic columns is evaluated by monitoring the column response to a tracer by use of a detector located at the column outlet. The quantities derived from these kind of experiments are gross parameters which stand for the overall column behaviour but fail to represent local contributions to the overall band broadening. For this reason, experimental techniques which allow for a locally resolved monitoring of band broadening inside the columns are desired to relate the underlying transport behaviour of the solvent flow to the overall macroscopic column performance.

In order to investigate local column properties, computed tomography (CT) as a non-invasive measurement technique was employed. CT-scanning is a modern technique deriving from medicine which is capable of monitoring the tracer fronts in situ. It can be used to gain inside into a variety of physical phenomena associated with transport in porous media [1-3]. The experiments were carried out using a reversed phase material (C18) packed into glass columns of different diameters. Water and methanol as well as solutions of potassium-iodide were used as mobile phases. The experimental results were fitted using the so called equilibrium dispersive model [4]. The additivity of the first and second moment was exploited to determine local axial dispersion coefficients.

One aim of this work was to evaluate the potential of computed tomography to give information about the local concentration profiles inside a chromatographic column. This information is relevant as the separation-efficiency of chromatographic columns strongly depends on a homogeneous structure of the packing. Furthermore, the results of this work shall contribute to gain a better understanding of the packing structures of adsorption columns and the influence of an uneven packing on the performance of the separation process. Long term goal is the implementation of the experimental results into spatially more dimensional models of adsorption processes.

Theory of adsorption

Hydrodynamic dispersion effects result in a limited efficiency of adsorption columns as the bands of the components to be separated spread. The dispersion is the result of convection as well as molecular diffusion. Convective dispersion is due to the microscopic velocity distribution caused by the adhesion at the surface of the adsorbent particles and the statistical backmixing associated with tortuous pathways through a packed bed.

The efficiency of the columns is determined by the degree of broadening of the band or front that is conveyed through the column. It is commonly quantified by parameters associated to the variance or second central moment σ^2 of the individual bands.

The efficiency or plate number N of a column is given by

$$N = \frac{(\mu_1)^2}{\sigma^2} \tag{1}$$

Where μ_1 is the first moment or mean residence time of the band. Another common term to describe the lumped effects of hydrodynamic dispersion is the height equivalent to a theoretical plate H. It is worth noticing that the efficiency as well as the equivalent plate height are not purely column characteristics but depend on the component of interest.

$$H = \frac{L}{N} \tag{2}$$

The equilibrium-dispersive model is a simple mass transfer model accounting for non idealities by means of a the so called apparent axial dispersion coefficient D_{ax}^{app}. It is frequently used for the design and optimization of adsorption processes, e.g in the field of chromatographic separations. The model bases on the assumption that the stationary and the mobile phase are in a permanent local equilibrium throughout the column. All non-idealities, including band-broadening due to mass transfer resistance are lumped into the apparent axial dispersion coefficient [4].

$$\frac{\partial c_i}{\partial t} + F \cdot \frac{\partial q_i^*}{\partial t} + u \cdot \frac{\partial c_i}{\partial z} = D_{ax}^{app} \cdot \frac{\partial^2 c_i}{\partial z^2} \tag{3}$$

The apparent axial dispersion coefficient is related to the variance of the eluting bands and can be determined from the equivalent plate height.

$$D_{ax}^{app} = u \cdot \frac{H}{2} \tag{4}$$

Theory of Computed Tomography

The measuring principle is based on the ability of x-rays to pass through almost all matter. During the transition the x-ray beams are attenuated following Lambert-Beer's law.

$$\ln\left(\frac{I}{I_0}\right) = \int_0^L -\mu \cdot dz \tag{5}$$

The intensity of the attenuated beams passing the object is monitored to obtain a projection of the object. From the projection data an image file that consists of an array

of CT numbers can be reconstructed. The CT-number is defined as a dimensionless attenuation coefficient in terms of SI-Units.

$$CT = \frac{\mu - \mu_{H_2O}}{\mu_{H_2O}} \tag{6}$$

For a porous object, the CT-number is given as the weighted mean of the CT-Number of the two phases, in particular the weighted mean of the CT-numbers of the fluid (or mobile) phase MP and the adsorbent (or stationary phase) SP. During a breakthrough experiment the mobile phase the column is initially saturated with ($MP1$) is displaced by another fluid ($MP2$) being either a different solvent or having a distinct composition. The mobile phase saturation S is given by the volume fraction of the corresponding mobile phase. The CT-Number during the duration of the breakthrough is given by [5]

$$CT(t) = \varepsilon \cdot [S_{MP1} \cdot CT_{MP1} + S_{MP2} \cdot CT_{MP2}] + [(1-\varepsilon) \cdot CT_{SP}] \tag{7}$$

Consequently the local saturations S during a breakthrough can be determined from three CT images representing the saturated state and the breakthrough. Furthermore, it must be assured that the CT-numbers of the pure mobile phases $MP1$ and $MP2$ are known and that their contrast in the attenuation coefficient is sufficiently large.

Experimental

The experimental setup used for the measurements is shown in figure 1. A high pressure gradient system consisting of two double piston HPLC pumps delivered pure solvent (MP1) and the solvent/ potassium iodide solutions (MP2), respectively. Methanol or water were used as solvents. Potassium iodide (KI) was chosen as the tracer component due to the high atomic mass of iodine which allows for a good contrast in the CT images.

A six port valve allowed for the mobile phase transition. The column was mounted to the patient table of the CT scanner. This rendered it possible to shift the column along its axis during the experiments. During each of the frontal analysis experiments the breakthrough behaviour of the front was monitored in different column cross sections. After each experimental run, the column was equilibrated before the images of the

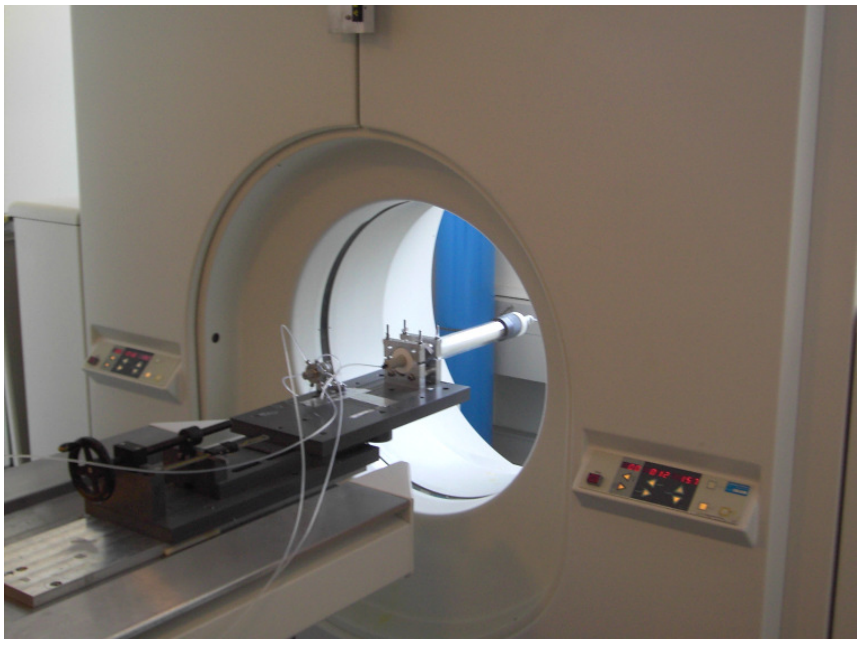

Figure 1: Experimental setup

saturated state were taken at all monitoring positions. A flow meter was used to observe the flow stability of the pumps.

Two axial compression columns made of glass having different dimensions were investigated. Steel columns could not be used for the reason that steel causes artefacts in the CT images. The columns were packed with a polydisperse, hydrophobic ODS phase. A non polar system was used to reduce interactions between the ionic tracer and the adsorbent to a minimum. Both columns were slurry packed with isopropanol as the pushing solvent.

Table 1: Column characteristics

column #	inner diameter [mm]	packing length [mm]
ID 26	26	240
ID 50	50	350

The CT Scanner used for the experiments was a Siemens Somatom plus 4th Generation Scanner.

Results and discussion

Exemplary images of the intra column breakthrough behaviour are shown in figure 2. The concave shape of the band is at least partially caused by the fact that transporting the tracer to the wall region of the columns takes additional time. Thus the concentration front close to the wall falls behind during the distribution process.

Intra column breakthrough curves were determined from the CT images. Results for the 50mm column are given in figure 3. As to be expected, the tracer bands were continuously spreading while progressing through the columns giving rise to a monotonic increase of the variance σ^2 of the bands.

The equilibrium dispersive model (EDM) was fitted to the experimental data. During the fitting procedure optimizing the least squares in tracer saturation, the local Peclet

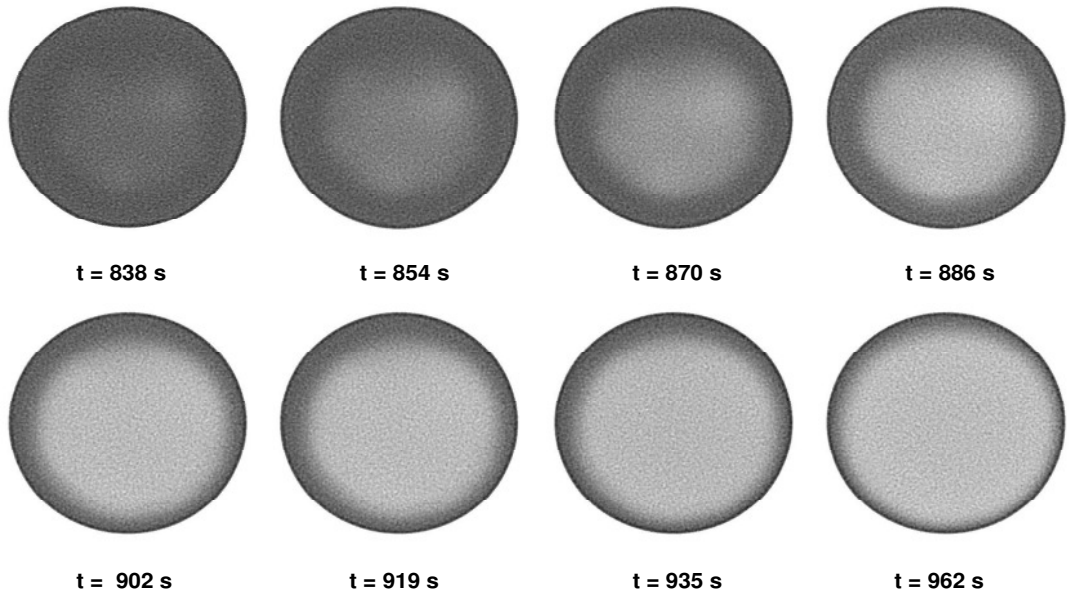

Figure 2: Intra column breakthrough of KI-solution for ID 26 at z/L = 0.35

number $Pe_z = u \cdot z / D_{ax}^{app}$ and the local retention time of the front t_z^R were varied. Representatives of the matched curves are shown together with the experimental data in figure 3.

The fitted curves represent the experimental points principally well with the exception of the very beginning and the very end of the graphs. In these regions deviations from the experimental curves can be found at some axial positions. This is likely to be due to non uniformities of the column packing.

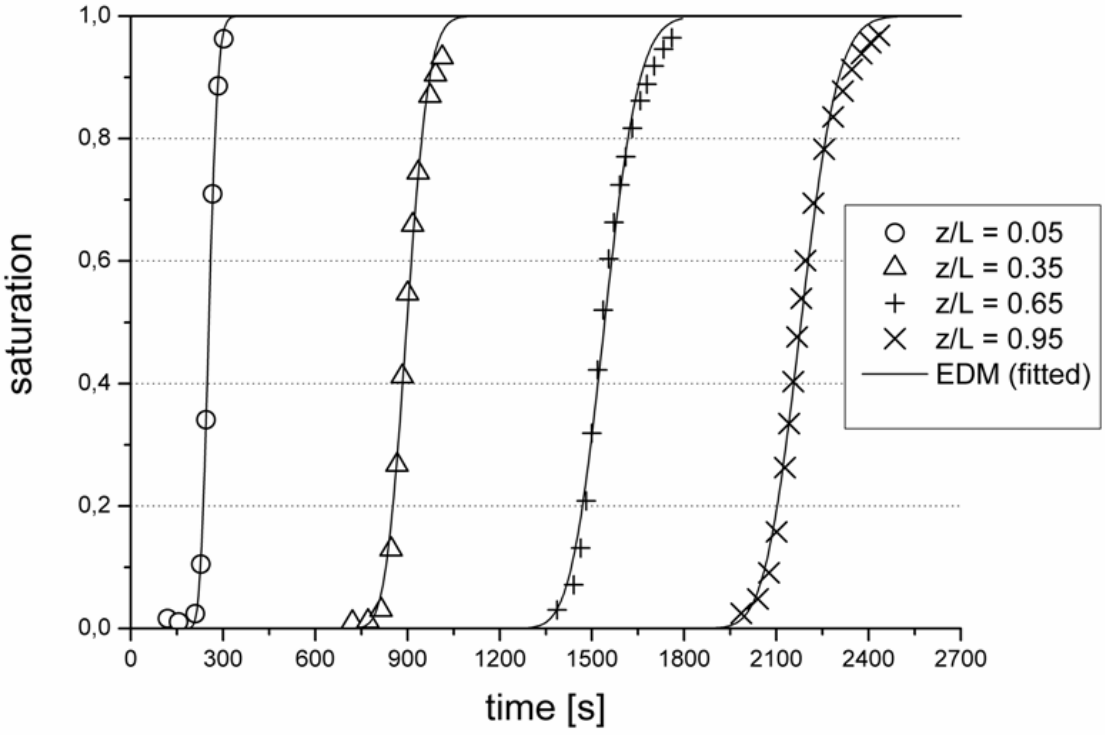

Figure 3: Experimental and fitted intra column breakthrough curves for ID 50 at different axial positions

In order to investigate the homogeneity and the radial dependency of the column properties, the column cross sections were equidistantly (with respect to the columns radius) subdivided into ten annulus. Subsequently the EDM was fitted to the breakthrough curves corresponding to each of the annulus segments. A representative of the results is given in figure 4 showing the matched breakthrough curves in the column centre and in the vicinity of the wall at different axial positions in the 50mm column.

It is evident that the bands travel faster in the central region than in the wall region of the column. It can be concluded that the column packing is less dense and offers a higher permeability in the core of the column compared to the column wall. This allows for higher migration velocities in the central region of the investigated columns. Moreover, the concentration profile close to the column wall has much stronger spread than the corresponding saturation profile in the column core. Obviously the efficiency in the wall region of the column is significantly lower. Similar results were obtained in all experiments.

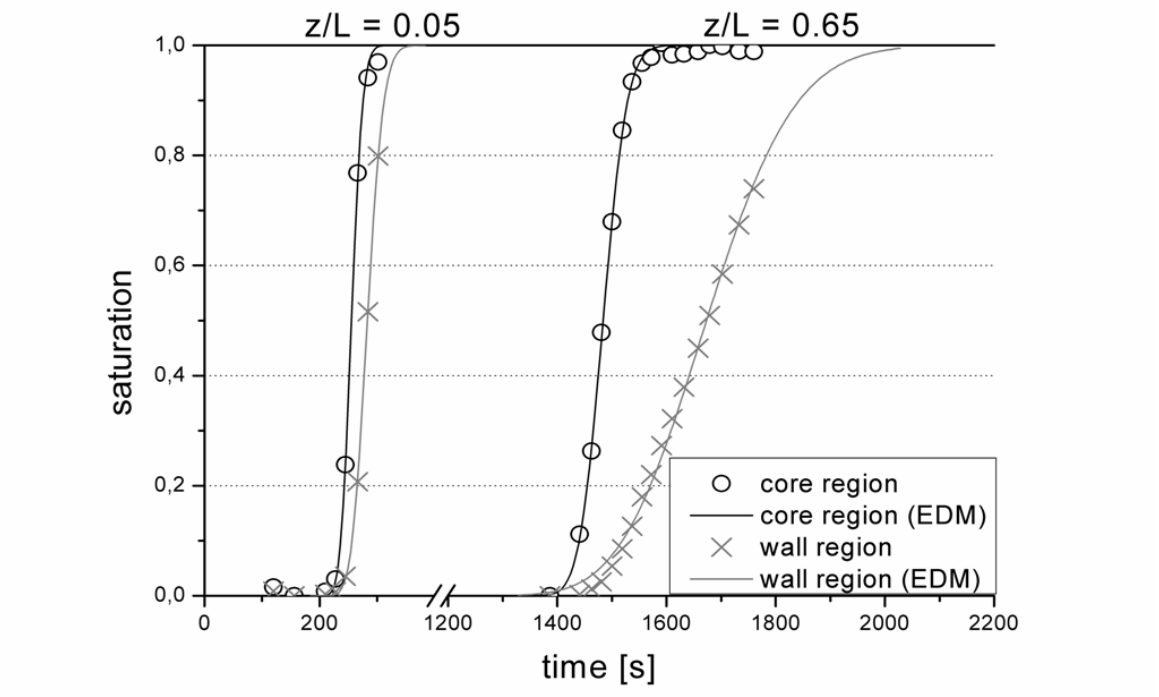

Figure 4: Comparison of the breakthrough behavior in the column core and close to the column wall, respectively (ID = 50mm)

The dependency of the column efficiency on the radial position was investigated closer by comparing the order of magnitude of the apparent dispersion coefficients of the annulus segments. It should be noted that the dispersion coefficient is proportional to the reciprocal of the efficiency. The trend is shown in figure 5.

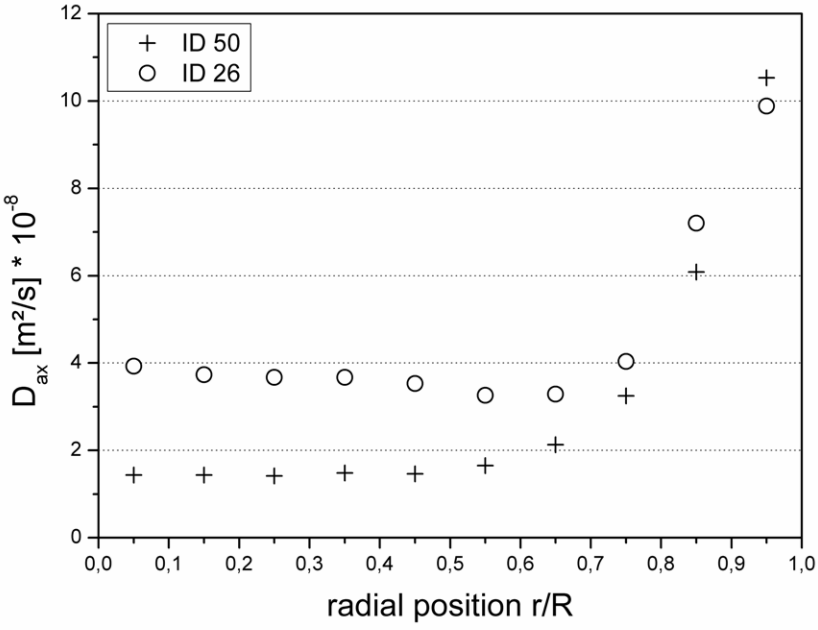

Figure 5: Dependency of the axial dispersion coefficient on the radial position

Either column exhibited an almost constant efficiency in the central region of the packing. Beyond this uniform region the efficiency was monotonically decreasing towards the column wall. In the adjacency of the columns wall, the dispersion coefficients were up to five times larger in comparison to the homogenous core region.

Conclusions

X-ray computed tomography was used to observe the breakthrough behaviour and efficiencies of adsorption columns made of glass in situ. The measurement technique proved itself to be a well suited tool for the non invasive characterisation of these kinds of columns.

Although we must caution regarding the interpretation of results based on a limited number of columns investigated, evidence was found that the properties of the packing are not evenly distributed within the column. The packed beds under investigation offered a denser and less efficient wall region compared to the column core. This is in good agreement with earlier findings [6] providing additional evidence that the porous bed in slurry packed columns is heterogeneous in the radial direction.

References

[1] J. Chaouki et al.; Ind. Eng. Chem. Res. 36 (1997) 4476-4503

[2] E. Peters et al.; J. Pet. Sci. Eng. 15 (1996) 23-31

[3] C. Karacan et al.; Chem. Eng. Sci. 58 (2003) 4681-4693

[4] G. Guiochon et al.; Modeling for preparative chromatography; Academic Press (2003)

[5] Kantzas; A.; AIChE J. 40 (1994) 1254-1261

[6] G. Guiochon et al.; J. Chromatogr. A 762 (1997) 83-88